Influence of Upconversion and Excited state absorption on the performance of an Erbium-Ytterbium doped DFB Fiber Laser

Justice Mpoyo Sompo
Department of Electrical and Electronic Engineering Science
University of Johannesburg
Johannesburg, South Africa
justice.sompo@gmail.com

Michael Grobler
Departement of Electrical and Electronic Engineering Science
University of Johannesburg
Johannesburg, South Africa
michaelg@uj.ac.za

Jean-Jacques Monga Kaboko
line 2: *Department of Electrical and Electronic Engineering Science*
University of Johannesburg
Johannesburg, South Africa
mongatvch@gmail.com

***Abstract*—Cooperative up-conversion and excited state absorption are the main limiting factors of short cavity erbium-ytterbium doped fiber lasers like DFB fiber lasers. In this report we quantify the influence of these detrimental effect by numerical modelling. The results of our analysis demonstrate that cooperative upconversion account for almost 10% in reduction of the laser output power. In addition, laser threshold and slope efficiency of the laser are also strongly influenced by cooperative upconversion and excited state absorption.**

Keywords—DFB, fiber Optic, Fiber Laser, Upconversion, Excited State Absorption.

I. INTRODUCTION

Rare earth doped Distributed Fiber (DFB) fiber lasers are an interesting type of fiber laser because of their unique characteristics like mode-hope, free robust single longitudinal mode operation, low frequency noise and high signal to noise ratio [1]. These unique features make them the most preferred candidates for a range of application such as, telecommunication [2-4] or sensing [5-7].

In a DFB fiber laser, gain is provided by a rare earth doped fiber and feedback is accomplished via a fiber Bragg grating (FBG) printed throughout this rare earth doped gain medium. Due to the foregoing reason, the cavity of a DFB fiber laser is often no longer than a few centimeters. To achieve significant gain inside such a short distance, high rare earth ion concentration is often required. Such high rare earth ion concentration leads inevitably to detrimental effects such as cooperative upconversion and exited state absorption, therefore luminosity quenching occur because of the erbium ions, limiting the gain of the laser. To increase the erbium ion concentration while avoiding these detrimental effects, solutions like using aluminum fiber and co-doping erbium with ytterbium ions, have been used. However even using these solutions, cooperative upconversion and excited state absorption still exist. Knowing the exact influence of these effects on the performance of a DFB fiber laser will be beneficial in designing such devices.

Multiple numerical modeling of Erbium and Erbium-Ytterbium DFB fiber lasers have been presented [8-11]. However, to the best of our knowledge, none of these attempts to quantify the detrimental effects in Erbium-Ytterbium DFB fiber lasers have been investigated sufficiently. In this paper we use a numerical model, based on rate equations to simulate DFB fiber laser behaviour. First, we take into account the detrimental effect of cooperative upconversion and excited state absorption. Following that we model the DFB fiber laser without these effects. The results of the two simulations are compared to provide a difference between the two and quantify the influence of these effects.

II. MATHEMATICAL MODEL

The Er^{3+}-Yb^{3+} co-doped medium is described by a set of rate equations derived from the transition between energy levels due to ion-ion and ion-light interaction. The ion–ion interactions that were considered were cooperative upconversion (CUP) among Er^{3+}-ions and energy transfer between Er^{3+}- and Yb^{3+}-ions. Ion-light interactions included absorption at the ground state, stimulated emission, and absorption at excited states (ESA). In addition to these transitions, spontaneous emission and non-radiative decays were also considered. The following rate equations were used to model the respective population densities:

$$\begin{aligned}\frac{\partial N_1}{\partial t} = {} & W_{21}N_2 + A_{21}N_2 + A_{41}N_4 \\ & + Ktr_{35}N_3N_5 \\ & + C_{up2}N_2^2 + C_{up3}N_3^2 \\ & - W_{13}N_1 - W_{12}N_1 \\ & - Ktr_{61}N_6N_1\end{aligned} \tag{2.1}$$

$$\begin{aligned}\frac{\partial N_2}{\partial t} = {} & W_{12}N_1 - W_{21}N_2 - C_{ESA23}N_2 \\ & - A_{21}N_2 + A_{32}N_3 \\ & - 2C_{up2}N_2^2\end{aligned} \tag{2.2}$$

$$\begin{aligned}\frac{\partial N_3}{\partial t} = {} & W_{13}N_1 - W_{21}N_3 + C_{ESA23}N_2 \\ & - C_{ESA34}N_3 \\ & - (A_{32} + A_{31})N_3 \\ & + A_{43}N_4 + C_{up2}N_2^2 \\ & - 2C_{up3}N_3^2 \\ & + Ktr_{61}N_1N_6 \\ & - Ktr_{35}N_3N_5\end{aligned} \tag{2.3}$$

$$\frac{\partial N_4}{\partial t} = C_{ESA34}N_3 - (A_{41} + A_{43})N_4 + C_{up3}N_3^2 \quad (2.4)$$

$$\frac{\partial N_5}{\partial t} = W_{65}N_6 - W_{56}N_5 - Ktr_{35}N_3N_5 + Ktr_{61}N_1N_6 \quad (2.5)$$

$$N_{Er} = N_1 + N_2 + N_3 + N_4 \quad (2.6)$$

$$N_{Yb} = N_5 + N_6 \quad (2.7)$$

In these equations:

$$W_{ij} = \frac{\sigma_{ij}I}{h\nu} \quad (2.8)$$

$$C_{ESA23} = \frac{\sigma_{23}I}{h\nu_s} \quad (2.9)$$

$$C_{ESA34} = \frac{\sigma_{34}I}{h\nu_p} \quad (2.10)$$

Where i and j represent the two energy levels involved in the transition and σ_{ij} the absorption or emission cross section of these transitions. N_i represents the population density of rare earth ions at different energy levels. Parameters used in the simulation are presented in table 1.

TABLE I.

symbol	Parameter	value	reference
σ_{12}	Er^{3+} absorption cross section at λ_s	8.9 x 10^{-25} m^2	[12]
σ_{13}	Er^{3+} absorption cross section at λ_p	2 x 10^{-25} m^2	[13]
σ_{21}	Er^{3+} emission cross section at λ_s	8.7 x 10^{-25} m^2	[12]
σ_{31}	Er^{3+} emission cross section at λ_p	2 x 10^{-25} m^2	[13]
σ_{56}	Yb^{3+} absorption cross section at λ_p	8.7 x 10^{-25} m^2	[14][15]
σ_{65}	Yb^{3+} emission cross section at λ_p	11.6 x 10^{-25} m^2	[16]
σ_{23}	ESA cross section of Er^{3+} at λ_s	1 x 10^{-27} m^2	[17]
σ_{34}	ESA cross section of Er^{3+} at λ_p	1 x 10^{-27} m^2	[17]
A_{21}	Spontaneous Emission rate of Er^{3+}	100 s^{-1}	[18][19]
A_{32}	Er^{3+} nonradiative decay from 3 to 2	10^5 s^{-1}	[20]
A_{41}	Spontaneous Emission rate of	10^5 s^{-1}	[20]
A_{43}	Er^{3+} nonradiative decay from 4 to 3	100 s^{-1}	[20]
C_{up2}	Cooperative upconversion coefficient from 2	2.5 x 10^{-21} m^3s^{-1}	[21,22]
C_{up3}	Cooperative upconversion coefficient from 3	2.5 x 10^{-21} m^3s^{-1}	[21,22]
Ktr_{35}	Energy transfer coefficient from Er^{3+} to Yb^{3+}	5 x 10^{-21} m^3 s^{-1}	[23],[22]
Ktr_{61}	Energy transfer coefficient from Yb^{3+} to Er^{3+}	5 x 10^{-21} m^3 s^{-1}	[21],[23],[22]
N_{Er}	Erbium ions density	1.2 x 10^{25} m^{-3}	-
N_{Yb}	Ytterbium ions density	2.4 x 10^{26} m^{-3}	-
λ_p	Pump wavelength	980 nm	-
λ_s	Laser wavelength	1550 nm	-
L	DFB Fiber Laser cavity length	50 mm	-
Γ_p	Overlap factor at pump wavelength	0.83	-
Γ_s	Overlap factor at signal wavelength	0.64	-
α_p	Background loss at pump wavelength	0.20 m^{-1}	-
α_s	Background loss at signal wavelength	0.15 m^{-1}	-
n_{eff}	Core effective refractive index	1.47	-
r	Core radius	2.3 µm	[24]
Δ	Index difference	9.3 x 10^{-3}	-

[a.] Sample of a Table footnote. (*Table footnote*)

Fig. 1. Example of a figure caption. (*figure caption*)

Equations (1) to (7) are solved for N_i in steady state for continuous wave operation. This means that all derivatives with respect to time will vanish. The resulting system is a nonlinear algebraic set of equations. It can be solved numerically by means of a Newton Raphson method or any other appropriate algorithm . In addition to these equations, propagation of the optical field in the periodic grating structure is modelled using a system of coupled mode equations. These equations describe two counter propagating optical fields inside the periodic structure created by the fibre Bragg grating. These fields feed energy to each other as they propagate due to the presence of the FBG. In addition, their respective intensity grow because of the presence of gain in the fiber cavity. The coupled equations are:

$$\frac{dR}{dz} = (g - i\hat{\sigma})R(z) - ikS(z) \quad (2.11)$$

$$\frac{dS}{dz} = -(g - i\hat{\sigma})S(z) - ik^{*}R(z) \quad (2.12)$$

In these equations R and S are the forward and backward propagating field given by:

$$R(z) = A(z)exp(-i\Delta\beta z + \phi/2) \quad (2.13)$$

$$S(z) = B(z)exp(i\Delta\beta z - \phi/2) \quad (2.14)$$

where k is the the "AC" (associated coupling) coefficient and $\hat{\sigma}$ is a general "DC" (demi coupling) self-coupling coefficient and g accounts for possible gain, e.g. in DFB fiber laser. In the case of a passive grating, $g = 0$.
The "DC" coupling coefficient is given by:

$$\hat{\sigma} \equiv \Delta\beta + \sigma - \frac{1}{2}\frac{d\phi}{dz} \quad (2.15)$$

Where $\Delta\beta$ is the detuning from the designed wavelength of an infinitesimally weak grating given by:

$$\Delta\beta = 2\pi n_{eff}\left(\frac{1}{\lambda} - \frac{1}{\lambda_B}\right) \quad (2.16)$$

Where λ_B is the Bragg wavelength given by $\lambda_B = 2n_{eff}\Lambda$ and $\frac{d\phi}{dz}$ accounts for the possible chirp of the grating period, and $\sigma = \frac{2\pi}{\lambda}\overline{\delta_{eff}}$ will vanish for weak gratings. These coupled equations are solved using the transfer matrix method to find R and S. The algorithm for solving the DFB fiber laser model can be explained as follow: For a given pump power an output power for the DFB fiber laser is estimated. The gain medium is divided in a number of equal sections (100 in our case). Knowing the input pump power at the first section and using the estimates signal output power, the gain is found from the population density at each energy level obtained from solving the rate equations for steady state. This process is repeated until the end of the DFB fiber laser cavity. At the end of the laser cavity a convergence condition is tested. If the convergence condition is satisfied, the process is stopped else, a secant shooting algorithm is used to refine the estimation, until convergence is achieved. Using this method we were able to compute the output power with respect to the pump power.

III. RESULTS AND DISCUSSION

The method used for quantifying cooperative upconversion and excited state absorption consists of solving the system model with and without the contribution of these phenomena. Results are then compared for different conditions like, pump power, phase shift position and grating coupling coefficient.

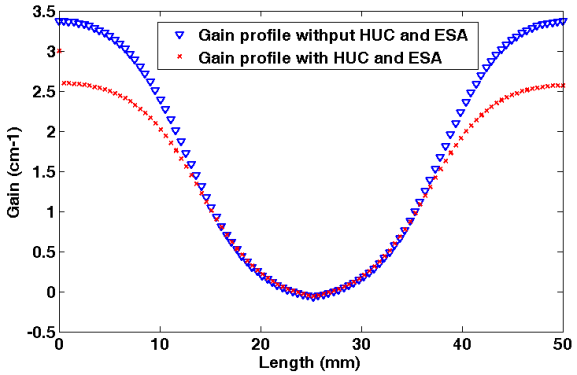

Fig. 1. Gain profile of DFB fiber laser simulated with and without HUC and ESA

Fig. 1 shows the gain distribution along the DFB fiber laser length. The minimum gain correspond to the location of the phase shift of the phase shifted FBG. It can be seen that the maximum gain is around 3.4 m^{-1} for the DFB fiber laser and this value drops to around 2.6 m^{-1} due to UC and ESA. This will inevitably result in a significant decrease in output power.

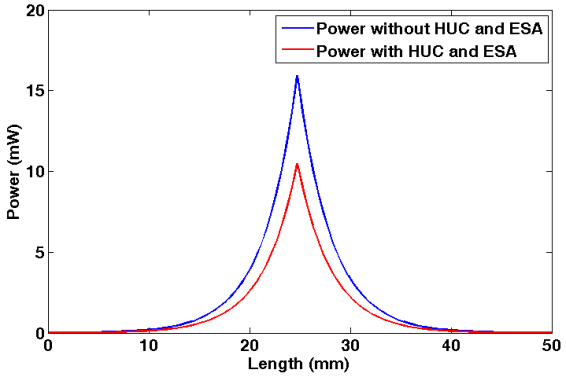

Fig. 2. Intensity distribution inside DFB fiber laser

The intensity distribution inside the DFB fiber laser is shown in Fig. 2. The peak corresponds to the location of the π phase shift in the FBG. Throughout the length of the laser, the intensity of the optical field is lower when UC and ESA are taken into account than when these phenomena are neglected.

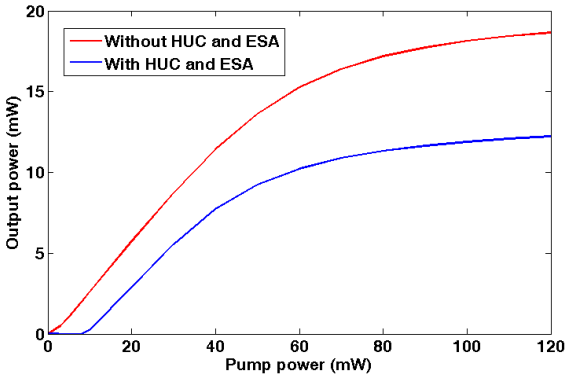

Fig. 3. Output power as a function of pump power of a DFB fiber laser with and without UC and ESA

The influence of UC and ESA can be seen in Fig. 3. Representing the output power as a function of the pump

power. It can be seen that UC and ESA increase the laser threshold from almost 1mW to close to 10 mW. Slope efficiency and output power are equally strongly reduced. Using a pump power of 120 mW in the simulation, an output power of 18.5 mW was achieve when UC and ESA were not taken into account. This value drops to 11.85 mW when these two phenomena were considered. The threshold is increased because, when the pump power is low, the rate of metastable level depopulation by ESA and UC is higher than the pump rate. Therefore population inversion is not achieved. When the pump power becomes sufficiently high, the pump rate becomes higher than the metastable level depopulation by ESA and UC, therefore oscillation can start.

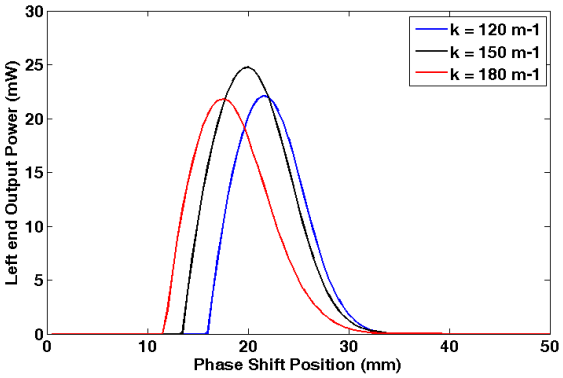

Fig. 4. Left end output power as a function of phase shift position

It can be shown that by placing the π phase shift FBG asymmetrically with respect to the ends of the DFB fiber laser, the output from the short arm can be an order of magnitude higher than that of the long arm [10]. However the phase shift cannot be moved completely towards one edge, because beyond a certain phase shift position the output power starts decreasing again. It means that there exists an optimum value of the phase shift position, corresponding to maximum output power. In our simulation this value was found to be 20.5 mm from the left end, if this end is considered to be the output. In addition, the output power depends also on the grating coupling coefficient. Fig.4. shows the optimum values of grating coupling coefficient and phase shift position obtained in our simulation. It can be easily seen that the optimum value for the coupling coefficient is 150 m^{-1}. However ESA and UC has no influence on these π phase shifted and coupling coefficient values.

IV. CONCLUSION

An Erbium-Ytterbium co-doped distributed feedback fibre laser was modelled. Simulations were performed and the influence of detrimental effects like cooperative up-conversion and excited state absorption were analysed using a numerical model and simulations. It was found that the influence of UC and ESA reduced the value of output power from 18.5mW to almost 12 mW for a pump power of 120 mW, thus reducing significantly the efficiency of the laser. The above shows that these phenomena cannot be neglected when designing a Distributed Feedback Fiber Laser.

REFERENCES

A. Suzuki, Y. Takahashi, M. Yoshida, M. Nakazawa, "An ultralow noise and narrow linewidth λ/4 shifted DFB Er-doped fiber laser with a ring cavity configuration," *IEEE Photon. Technol. Lett.*, vol. 19, no. 9, pp. 1463–1465, 2007

[2] J. Hubner, P. Varming, and M. Kristensen, "Five wavelength DFB fiber laser source for WDM systems," *Electron. Lett.*, vol. 33, no. 2, pp. 139-140, 1997.

[3] M. Ibsen, S. U. Alam, M.N. Zervas, A. B. Grudinin, and D. N. Payne, "8-and 16-channel all fiber DFB laser WDM transmitter with integrated pump redundancy," *IEEE Photon. Technol. Lett.*, vol. 11, no. 9, pp. 1114-1116, Sep. 1999.

[4] H. N. Poulsen, P. Varming, A. Buxens, A. T. Clausen, P. Munoz, P. Jeppesen, C. V. Poulsen, J. E. Pedersen, and L. Eskilsen, "1607 nm DFB fiber laser for optical communication in the L-band, "presented at the Eur. Conf. Optical Communication (ECOC), Nice, France, Sep 26-30, 1999, Paper MoB2.1.

[5] J. T. Kringlebotn, W. H. Loh, and R. I. Laming, "Polarimetric Er^{3+} -doped fiber distributed –feedback laser sensor for differential pressure and force measurements," *Opt. Lett*., vol. 21, no 22, pp. 1869-1871, 1996.

[6] E. Ronnekleiv, M. Ibsen, and G. J. Cowle, "Polarization characteristics of fiber DFB lasers related to sensing applications," *IEEE J. Quantum Electron*., vol. 36, no. 6, pp. 656-664, Jun. 2000.

[7] O. Hadeler, M. Ibsen, and M. N. Zervas, "Distributed-feedback fiber laser sensor for simultaneous strain and temperature measurements operating in the radio-frequency domain," *Appl. Opt*., vol. 40, no. 19, pp. 3169-3175, 2001.

[8] A. I. Azmi, D. Sen, and G. D. Peng, "Output power and threshold gain of apodized DFB fiber laser," *Proc. Of SPIE.*, vol. 7386 73860K

[9] J. del Valle-Hernandez, Y. O. Barmenkov, S. A. Kolpakov, and M. V. Andrés, "Effect of the Excited State Absorption on the efficiency of Erbium-Doped DFB Fiber Lasers," *Laser Physics.*, vol.22, no. 1, pp. 232-239

[10] Kuthan Yelen, Mikhail N, Zervas, and Louise M. B. Hickey, "Fiber DFB Lasers with Ultimate Efficiency," *J. Lightw. Technol*., vol. 23, no. 1, January 2005.

[11] Kuthan Yelen, Louise M. B. Hickey, and Mikhail N. Zervas, "Experimentally Verified Modeling of Erbium-Ytterbium Co-Doped DFB Fiber Lasers," *J. Lightw. Technol*., vol.23, no. 3, March 2005.

[12] L. W. Barnes, R. I. Laming, E. J. Tarbox and P. R. Morkel, " Absorption and emission cross section of Er^{3+} doped silica fiber*," IEEE J. Quantum Electron*., vol. 27, no. 4, pp. 1004-1010, Apr 1991.

[13] E. Desurvire, J. L. Zyskind and C. R. Giles, "Design optimization for efficient erbium-doped fiber amplifiers," *J. Lightw. Technol*., vol.8, no. 11, pp. 1730-1741, Nov. 1990.

[14] H. M. Pask, R. J. Carman, D. C. Hanna, A. C. Tropper, C. J. Mackechnie, P. R. Barber, and J. M. Dawes, "Ytterbium-doped silica fiber lasers: versatile sources for the 1-1.2 µm region, *" IEEE J. Select. Topics Quantum Electron.*, vol. 1. No. 1, pp. 2-13, Apr. 1995.

[15] X. Zou and H. Toratani, "Evaluation of spectroscopic properties of Yb^{3+} -doped glasses," *Phys. Rev. B, Condens. Matter*, vol. 52, no. 22, pp. 15889-15897, 1995.

[16] H. Yin, P. Deng, J. Zhang, and F. Gan, "Emission properties of Yb^{3+} in fluorophosphate glass," *J. Non-Cryst. Solids.*, vol. 210243-210248, 1997.

[17] J. Nilsson, P. Blixt, B. Jaskorzynka, and J. Babonas, "Evaluation of parasitic upconversion mechanisms in Er^{3+} -doped silica-glass fiber by analysis of fluorescence at 980 nm," J. Lightw. Technol., vol. 13, no. 3, pp. 341-349, 1995.

[18] E. Desurvire, C. R. Giles, and J. R. Simpson, "Gain saturation effects in high-speed, multichannel Erbium-doped fiber amplifiers at lambda = 1.53 µm," J. Lightw. Technol., vol. 7, no. 12, pp. 2095-2104, Dec. 1989.

[20] C. Jiang, W. Hu, and Q. Zeng, "Improved gain performance of high concentration Er^{3+}-Yb^{3+}codoped phosphate fiber amplifier," *IEEE J. of Quantum. Electron.*, vol. 41, no. 5, pp. 704-708, 2005.

[21] B. Hwang, S. Jiang, T. Luo, J. Watson, G. Sorbello, and N. Peyghambarian, "Cooperative upconversion and energy transfer of new high Yb^{3+} -Er^{3+} doped phosphate glasses," J. Opt. Soc. Amer. B, Opt. Phys., vol. 17, no. 5, pp. 833-838, 2000.

[22] S. Taccheo, G. Sorbello, S. Longhi, and P. Laporta, "Measurement of the energy transfer and upconversion constants in Er-Yb-doped phosphate glass," Optical Quantum Electron., vol. 31, pp 249-262, 1999.

[23] C. Lester, A. Bjaklev, T. Rasmussen, and P. G. Dinessen, "Modeling of Yb^{3+} senzitised Er^{3+} doped silica waveguide amplifiers," J. Lightw. Technol., vol. 13, no. 5, pp. 740-743, May 1995.